International Journal of Radiation Oncology biology • physics

www.redjournal.org

Biology Contribution

Regulatory T Cells Shape the Differential Impact of Radiation Dose-Fractionation Schedules on Host Innate and Adaptive Antitumor Immune Defenses

Joseph Sia, MB ChB, FRANZCR, PhD,*,†,‡ Jim Hagekyriakou, PhD,§ Ioana Chindris, HSc,*,† Hassan Albarakati, MSc,§ Trevor Leong, MBBS, MD, FRANZCR,†,‡ Ramona Schlenker, PhD,|| Simon P. Keam, PhD,†,¶,# Scott G. Williams, MBBS, BScMed, FRANZCR, MD,‡ Paul J. Neeson, PhD,†,# Ricky W. Johnstone, PhD, FAHMS,*,† and Nicole M. Haynes, PhD*,†

**Translational Hematology Program, Peter MacCallum Cancer Centre, Melbourne, Australia; †Sir Peter MacCallum Department of Oncology, The University of Melbourne, Parkville, Australia; ‡Radiation Oncology Department, Peter MacCallum Cancer Centre, Melbourne, Australia; §Physical Sciences Department, Peter MacCallum Cancer Centre, Melbourne, Australia; ||Roche Pharmaceutical Research and Early Development, Roche Innovation Centre Munich, Penzberg, Germany; ¶Tumour Suppression Laboratory, Peter MacCallum Cancer Centre, Melbourne, Australia; and #Cancer Immunology Research Program, Peter MacCallum Cancer Centre, Melbourne, Australia*

Received Feb 19, 2021; Revised May 4, 2021; Accepted for publication May 13, 2021

Purpose: We examined how radiation dose per fraction (DPF) and total dose, as represented by biological effective dose (BED), can independently and differentially affect the immunomodulatory capacity of radiation therapy (RT).

Corresponding author: Nicole M. Haynes, PhD; E-mail: nicole.haynes@petermac.org

Ricky W. Johnstone and Nicole M. Haynes made equal contributions to this study.

Work from the Johnstone laboratory was supported by the imCORE Network on behalf of F. Hoffmann-La Roche Ltd (R.W.J. and N.M.H.), the Cancer Council Victoria, National Health and Medical Research Council of Australia (NHMRC) and The Kids' Cancer Project (R.W.J.), the II-ON network on behalf of Bristol Myers Squibb (N.M.H.), the Australian Government Research Training Program Scholarship and the Royal Australian New Zealand College of Radiologists (RANZCR) Withers and Peters Grant (J.S.).

Disclosures: R.S. is a current employee of F. Hoffmann-La Roche Ltd. The laboratory of R.W.J. receives research support from F. Hoffmann-La Roche Ltd., Bristol Myers Squibb, AstraZeneca, and MecRx. R.W.J. is a scientific consultant and shareholder in MecRx. N.M.H. is a shareholder in CTxONE Pty Ltd.

Data Sharing Statement: All RNAseq data files have been deposited into the Gene Expression Omnibus under accession number GSE162418.

Supplementary material associated with this article can be found in the online version at doi: https://doi.org/10.1016/j.ijrobp.2021.05.014.

Acknowledgments—We would like to thank Drs Maria Doyle, Niko Thio, Simon Hogg, and Stephin Vervoort for helpful discussion relating to RNA sequencing analysis. We also acknowledge the generous support of The Peter MacCallum Foundation and Australian Cancer Research Foundation.

Int J Radiation Oncol Biol Phys, Vol. 000, No. 00, pp. 1–13, 2021

https://doi.org/10.1016/j.ijrobp.2021.05.014

Methods and Materials: AT3-OVA mammary and MC38 colorectal tumors in C57BL/6 mice were irradiated with rationally selected dose-fractionation schedules, alone or with immune-modulating or -depleting agents. Tumor growth was monitored as a readout of therapeutic response. Flow cytometry and RNA sequencing of mouse tumors and analysis of transcriptomic data sets from irradiated human cancers were used to examine the immunomodulatory effects of the different radiation schedules.

Results: In AT3-OVA tumors, radiation DPF rather than BED determined the ability of RT to evoke local antitumor $CD8^+$ T cell responses and synergize with anti-PD-1 therapy. Natural killer cell−mediated control of irradiated tumors was more sensitive to radiation BED. Radiation-induced regulatory T cell (Treg) responses, which were detected in both mouse and human tumors, were a major factor underlying the differential activation of adaptive immunity by radiation DPF and the activity of natural killer cells during the early phase of response to RT. Targeted inhibition of Treg responses within irradiated tumors rescued and enhanced local tumor control by RT and permitted the generation of abscopal and immunologic memory responses, irrespective of radiation schedule. MC38 tumors did not support the induction of an amplified Treg response to RT and were highly vulnerable to its immunoadjuvant effects.

Conclusions: Local radiation-induced Treg responses are influenced by radiation schedule and tumor type and are a critical determinant of the immunoadjuvant potential of RT and its ability to synergize with T cell−targeted immunotherapy.

Introduction

Radiation therapy (RT) is a well-established cancer treatment modality in the modern armamentarium against cancer. In addition to its ability to directly kill tumor cells, RT also has pleiotropic effects on the immunogenic status of the tumor microenvironment, influencing host antitumor immune defenses within and outside (abscopal effect) the irradiated volume.[1,2] In recent years, the range of radiation dose-fractionation schedules used in the clinic has significantly broadened due to increased adoption of SABR.[3,4] Radiation schedules used in SABR involve the delivery of high radiation doses in one or a few fractions (usually 6-30 Gy per fraction), in contrast to conventionally fractionated schedules that use a protracted number of daily low-dose fractions over many weeks (usually ≤4 Gy per fraction).

To date, only a few studies have used stringent functional analytics to examine the differential effects of radiation dose-fractionation schedules on host anticancer immunity.[5,6] Previous preclinical studies showed that radiation schedules of 8 Gy per fraction or less were more effective than a single fraction of 20 Gy in supporting the antitumor activity of checkpoint blockade immunotherapy in tumors growing outside the irradiated volume.[5,7] This abscopal activity of RT was linked to activation of stimulator of interferon genes (STING) and induction of type I interferon (IFN) release, leading to the maturation of type I conventional dendritic cells (cDC1s) and stimulation of T cell responses.[8-10] Single-fraction doses of more than 10 to 12 Gy were reported to increase tumor cell expression of the exonuclease TREX1, which degrades cytosolic dsDNA and in turn prohibits the activation of STING.[7] In contrast, another study showed that a single fraction of 20 Gy could evoke STING activation in circulating dendritic cells, resulting in the induction of antitumor $CD8^+$ T cell responses.[11] The somewhat contradictory findings of the 2 studies, which used different in vivo models, raised the question of whether tumor microenvironmental factors may also play a role in influencing the effectiveness of RT to act as an in situ vaccine.

In this study, the differential effects of radiation dose-fractionation schedules on the ability of RT to engage $CD8^+$ T and natural killer (NK) cell−mediated antitumor responses, independent of immunotherapy, were examined in a C57BL/6 syngeneic model of triple negative breast cancer. Rationally selected radiation schedules, based on the radiation response curve of the tumor cells, were used to distinguish the effects of dose per fraction (DPF) from those of biological effective dose (BED) on the immunoadjuvant potential of RT. We found that induction of $CD8^+$ T cell activity was regulated by radiation DPF rather than BED, whereas induction of NK cell responses required a sufficiently high radiation BED that was independent of DPF. Central to the modulation of these responses was the DPF-dependent effects of RT on the accumulation of regulatory T cells (Tregs) within irradiated tumors. Targeted inhibition of radiation-induced Treg responses enhanced the local curative effects of RT and permitted the induction of abscopal and immunologic memory responses. Together, these findings establish that Tregs are a dominant tumor cell−extrinsic determinant of the immunoadjuvant potential of RT.

Methods and Materials

Cell lines

The AT3 cell line was generated from an autochthonous mammary carcinoma isolated from a C57BL/6 MMTV-PyMT transgenic mouse[12] and retrovirally transduced to express ovalbumin.[13] The MC38 colon adenocarcinoma cell line was obtained from American Type Culture

Collection. These cell lines were cultured as outlined in Methods E1 and confirmed mycoplasma negative by polymerase chain reaction analysis. Radiation cell survival curves were generated using clonogenic assays as described by Franken et al[14] and detailed in Methods E2.

In vivo mouse experiments

Animal studies were performed with approval from the Peter MacCallum Cancer Centre (PMCC) Animal Experimentation Ethics Committee (Melbourne, Australia). Female C57BL/6 mice were purchased from the Walter and Eliza Hall Institute (Melbourne, Australia). C57BL/6 Foxp3-DTR/EGFP (DEREG) and C57BL/6 Batf3$^{-/-}$ mice were bred in-house and genotyped at the PMCC. Mice were used at 6 to 12 weeks of age and maintained in the PMCC animal facility. We injected 1.8×10^6 AT3-OVA tumor cells orthotopically into the left 4th mammary fat pad or subcutaneously, and 1×10^6 MC38 tumor cells were injected subcutaneously. For study of the abscopal effect, AT3-OVA tumor cells were injected bilaterally into the left and right 4th mammary fat pads 7 days apart. Tumor growth was monitored using electronic calipers. Treatment of AT3-OVA and MC38 tumors started when they reached 25 to 35 mm^2 or 40 to 50 mm^2, respectively. Mice were euthanized when tumors reached 100 to 200 mm^2 or 40 to 100 days after treatment initiation.

Mouse tumor irradiation

Mice were anesthetized with a ketamine/xylazine mix and positioned on a Perspex plate covered by a 3 mm thick lead shield with 0.8 cm^2 openings for localized irradiation of the tumors. Irradiation was delivered using a 6 MeV electron beam from a clinical linear accelerator. Control mice were anesthetized but not irradiated.

In vivo treatments

Therapeutic antibodies were purchased from BioXCell unless specified. Antibodies to PD-1 (Clone: RMP1-14) and CTLA-4 (Clones: 9H10 and 9D9 D265A[15]) were injected intraperitoneally at a dose of 150 μg (first injection, day 0 relative to start of RT) followed by 100 μg on days 4, 8, 12 and 16, unless specified. Immune cell-depleting antibodies to CD8β (53-5.8) or asialo-GM1 (Wako Chemicals) were injected intraperitoneally at a dose of 100 μg from day 0 relative to the start of RT and every 3 to 4 days thereafter. Control mice were treated with a relevant isotype control. For experiments using DEREG mice, a single dose of diphtheria toxin (DT; 0.1 μg) was injected intraperitoneally to deplete Tregs.

Testing for the induction of immunologic memory

Spleens were harvested from AT3-OVA tumor-bearing C57BL/6 wildtype mice 2 - 8 weeks post treatment completion, processed into single-cell suspensions and red blood cell lysed. A single spleen preparation was intravenously injected equally across 2 treatment naïve C57BL/6 mice. Seven to 10 days after splenocyte transfer, one recipient was injected with AT3-OVA tumor cells and the other was injected with AT3-parental cells as described earlier.

Flow cytometry analysis of mouse tumors and tissues

Tumors, spleen, and lymph nodes were harvested, mechanically cut into small pieces, and collagenase IV digested (Worthington BioChem). Flow-Count Fluorospheres counting beads (Beckman Coulter) were added to the single-cell suspension. Pelleted cells were resuspended in cold FACS buffer supplemented with 2% normal mouse serum (Jackson ImmunoResearch). The cells were then stained with fluorescently labeled antibodies to immune biomarkers, listed in Methods E3. Data acquisition was performed with a BD FACSymphony (BD Biosciences) and analyzed using FlowJo software (Tree Star Incorporated).

Preparation of mouse RNA for sequencing

AT3-OVA tumors were harvested days 5 and 13 after completion of RT, processed into single-cell suspensions, and flow-sorted for CD45.2$^+$ cells. Samples were resuspended in QIAzol lysis reagent (QIAGEN), and RNA was extracted using the Direct-zol RNA MicroPrep kit (Zymo Research). RNA quality was assessed using the Aligent 2100 Bioanalyzer. Samples with an RNA integrity number of >8.5 were processed for library preparation and paired-end mRNA sequencing. Analysis of the RNA data sets was performed as described in Methods E4.

Human transcriptomic data sets

Publicly accessible human breast cancer transcriptomic data were downloaded from the Gene Expression Omnibus. A human prostate cancer data set was also used, with details of the patient cohort, sample collection, and analysis described by Keam et al.[16] Gene scores were calculated as described in Methods E5.

Statistics

Unless otherwise stated, unpaired 2-tailed Student's t test and log-rank test were used for group comparison and Kaplan-Meier survival analyses, respectively, using GraphPad Prism (version 8.3.1).

Results

Antitumor CD8$^+$ T and NK cell responses are differentially modulated by radiation dose-fractionation schedules

To select the radiation dose-fractionation schedules for study, the radiation cell survival curve of AT3-OVA mammary carcinoma tumor cells was generated using clonogenic survival assays (Fig. E1A). The α/β parameter of this tumor cell line, as based on the linear-quadratic model, was determined to be 16 Gy.[14] Because the total cytotoxic effect of a radiation schedule is not the arithmetic sum of the doses per fraction, BED was used as a surrogate of total dose for comparison between radiation schedules.[17] Based on prior work,[18] the 3 × 4 Gy and 1 × 20 Gy schedules were used as starting points for selection of comparative dose-fractionation regimens. Using the BED equation, the 9 × 4 Gy schedule (BED_{16} 45 Gy) had a BED similar to 1 × 20 Gy (BED_{16} 45 Gy) but the same DPF as 3 × 4 Gy (BED_{16} 15 Gy), thus serving as a control for BED and DPF between the 3 × 4 Gy and 1 × 20 Gy schedules (Fig. E1B). The 3 × 8 Gy (BED_{16} 36 Gy) and 1 × 12 Gy (BED_{16} 21 Gy) schedules were investigated to facilitate comparison with other published studies.[5,7]

The ability of each of these radiation schedules to control established orthotopic AT3-OVA tumors in wildtype C57BL/6 mice was examined (Fig. 1A). As expected, AT3-OVA tumors decreased in size after RT, and the period of sustained tumor control increased in a BED-dependent manner (Fig. 1B). To determine the contribution of CD8$^+$ T cells to the local antitumor effects of RT, mice were injected with depleting antibodies to CD8β (Fig. 1A). At the time of treatment, established AT3-OVA tumors were confirmed to be refractory to control by CD8$^+$ T cells (Fig. 1B). By contrast, in irradiated tumors, anti-CD8β treatment compromised tumor control when given with low-to-moderate DPF radiation schedules (3 × 4 Gy, 9 × 4 Gy, 3 × 8 Gy), but not high DPF schedules (1 × 12 Gy, 1 × 20 Gy; Fig. 1B). In line with these data, in *Batf3*$^{-/-}$ mice that lack cross-presenting cDC1s and the ability to prime CD8$^+$ T cell responses,[19] 3 × 4 Gy but not 1 × 20 Gy RT demonstrated a reduced capacity to control tumor growth (Fig. 1C). The impact of radiation DPF on CD8$^+$ T cell responses was further demonstrated by the finding that only radiation schedules shown to promote engagement of CD8$^+$ T cell responses could synergize with anti-PD-1 therapy in AT3-OVA tumor-bearing wildtype mice (Fig. 1D). Because the 9 × 4 Gy and 1 × 20 Gy schedules are isoeffective (having similar BED values) yet differed in their ability to engage CD8$^+$ T cell responses, this series of findings suggests that radiation DPF is a more critical parameter than BED in regulating CD8$^+$ T cell responses to RT.

In wildtype mice injected with NK cell–depleting anti-asialo-GM1 antibodies (Fig. 1A), the antitumor effect of the 9 × 4 Gy, 3 × 8 Gy, and 1 × 20 Gy schedules (BED_{16} 36-45 Gy), but not of the 3 × 4 Gy and 1 × 12 Gy schedules (BED_{16} 15-21 Gy), was compromised (Fig. 1E). Therefore, a radiation BED threshold of approximately 36 Gy was needed to evoke effective antitumor NK cell responses, a requirement that was independent of radiation DPF. Together, these findings establish that radiation-induced antitumor CD8$^+$ T and NK cell responses can be differentially modulated by DPF and BED (Fig. 1F).

RT induces enrichment of tumor-associated Tregs but not CD8$^+$ T cells

Factors underpinning the contrasting ability of the 3 × 4 Gy and 1 × 20 Gy schedules to engage host immune defenses were next explored. Flow cytometric analysis of irradiated AT3-OVA tumors revealed no differences in total CD8$^+$ T cell numbers with either schedule relative to mock RT (Fig. 2A). By contrast, significant increases in CD4$^+$ conventional T cell and Treg numbers were observed within the first 5 days post-RT in response to both schedules (Fig. 2B-D). Within the Treg compartment, radiation-induced increases in expression of Foxp3 and membrane-associated CTLA-4 and LAG-3 were identified, potentially indicative of enhanced regulatory function (Fig. E2A-B). The proportion of neuropilin-1 (Nrp1)$^+$ Tregs was also increased in response to both 3 × 4 Gy and 1 × 20 Gy RT (Fig. E2C), suggesting that the accumulation of Tregs post-RT was more likely due to newly recruited or expanded Tregs (Nrp1$^+$ natural Tregs) rather than in situ conversion from CD4$^+$ conventional T cells (Nrp1$^-$ induced Tregs).[20,21] NK cell numbers were also increased within the first 5 days post-RT in response to both schedules (Fig. 2E). The dynamics of tumor-associated T and NK cell numbers were synchronized to the completion, rather than commencement, of RT.

Differences in the kinetics and amplitude of tumor-associated T-cell responses between the 3 × 4 Gy and 1 × 20 Gy radiation schedules were only observed within the Treg compartment (Fig. 2C). Treg numbers peaked higher and earlier in 1 × 20 Gy-irradiated tumors. This difference was determined to be a function of radiation DPF rather than BED because the kinetics (Fig. 2D, left) and amplitude (Fig. 2D, right) of the Treg response to the 9 × 4 Gy schedule phenocopied that of 3 × 4 Gy, not 1 × 20 Gy.

By day 13 post-RT, T cell numbers had contracted back to mock RT levels in both the 3 × 4 Gy and 1 × 20 Gy-irradiated tumors (Fig. 2A-C). However, in 1 × 20 Gy-irradiated tumors, NK cell numbers remained significantly elevated at days 13 and 21 relative to the mock and 3 × 4

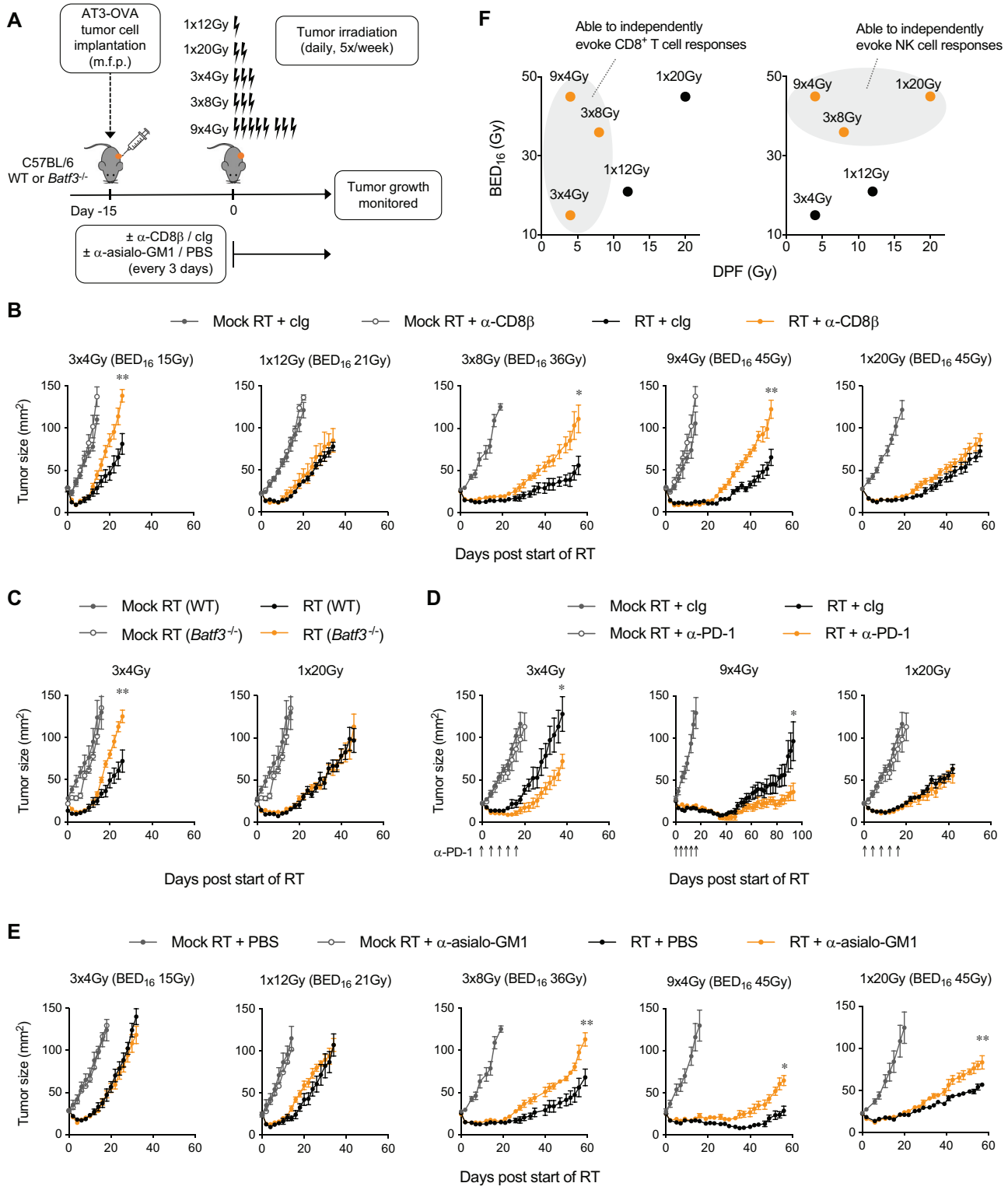

Fig. 1. Differential effects of radiation dose fractionation on antitumor immune responses in AT3-OVA tumors. (A) Schema of experimental approach. (B-E) Growth of irradiated and mock-irradiated AT3-OVA tumors (B) wildtype (WT) mice depleted of $CD8^+$ T cells; (C) $Batf3^{-/-}$ and WT mice; (D) WT mice treated with anti-PD-1 antibodies, as indicated by arrows; (E) WT mice depleted of NK cells. n = 4 to 6 mice/group; data representative of 2 independent experiments. Data presented as mean ± standard error of the mean. *P < .05, **P < .01. (F) Representation of radiation schedules capable of evoking antitumor $CD8^+$ T and NK cell responses.

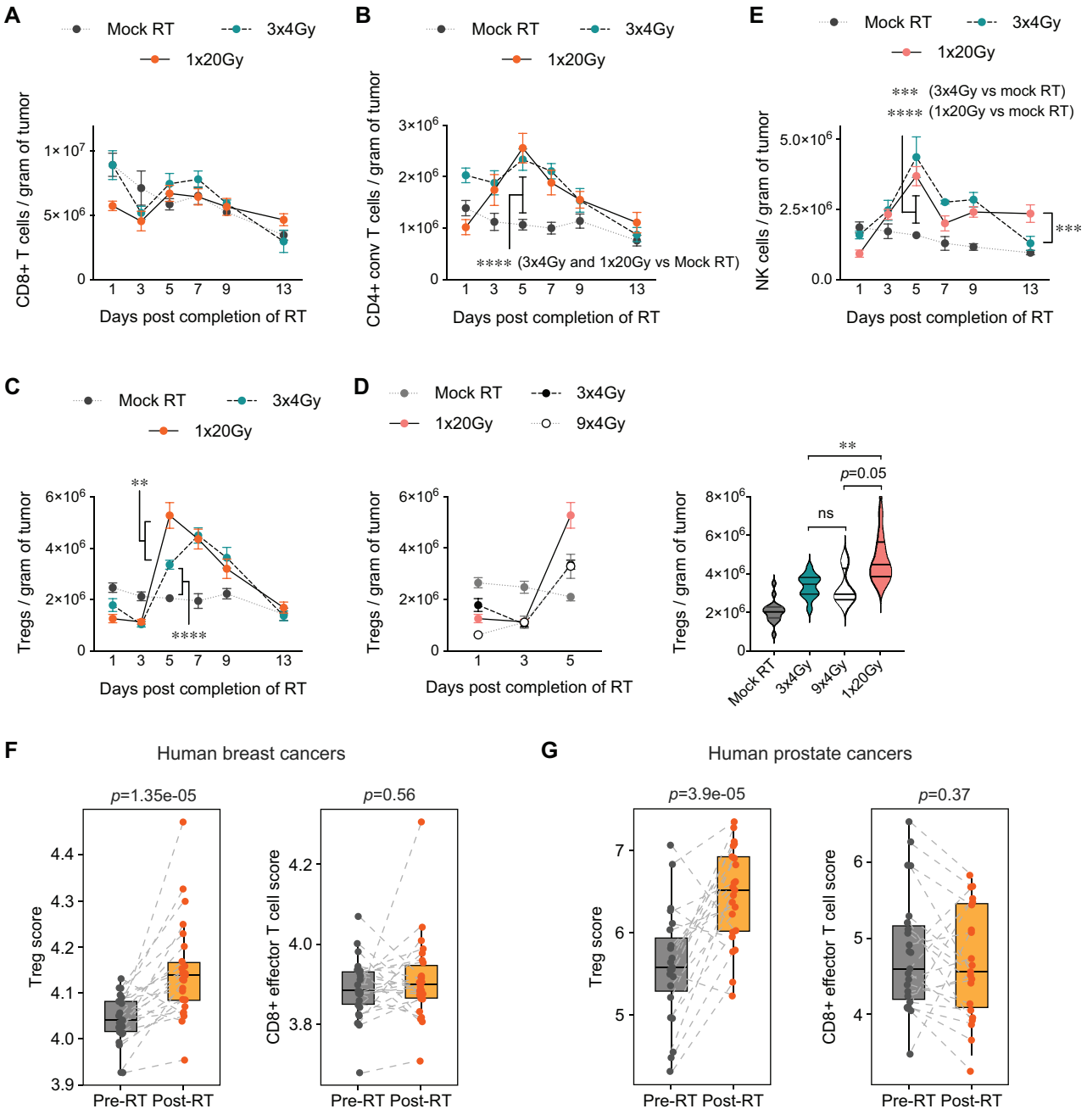

Fig. 2. Differential modulation of CD8$^+$ T cells and Tregs by high-DPF RT in mouse and human tumors. (A-C and E) Absolute numbers of tumor-associated (A) CD8$^+$ T cells, (B) CD4$^+$ conventional T cells, (C) Tregs, and (E) NK cells. (D) Absolute numbers of tumor-associated Tregs (left); day 5 data from this graph are presented in a violin plot (right). (A-E) n = 4 to 17 mice/group, combined from 4 independent experiments. Data presented as mean ± SEM; NS = nonsignificant. $^{**}P$ <.01, $^{***}P$ <.005, $^{****}P$ <.001. (F and G) Radiation-induced modulation of Treg and CD8$^+$ T cell gene scores in human (F) breast and (G) prostate cancers. Boxes and whiskers are plotted using the Tukey method. Dotted lines connect paired samples.

Gy-irradiated tumors (Fig. 2E and Fig. E3). The persistence of NK cells after contraction of the Treg response in 1 × 20 Gy-irradiated tumors may explain the delayed effect of anti-asialo-GM1 treatment on tumor growth after 1 × 20 Gy RT (Fig. 1E).

In line with the T cell changes observed in AT3-OVA mammary tumors, analysis of a publicly available transcriptomic data set of 52 paired human breast cancer samples obtained pre- and post-RT (GSE65505)[22] revealed marked induction of a Treg

signature (*FOXP3, IL2RA, IL2RB*, and *TNFRSF1B*[23]) within 10 days after 1 × 15-21 Gy RT (Fig. 2F). A $CD8^+$ effector T cell signature (*CD8A, CD8B, IFNG,* and *PRF1*[24]) was nonetheless unchanged (Fig. 2F). To corroborate these findings, an independent set of 46 paired human prostate cancer biopsies collected before and 14 days after 1 × 10 Gy high-dose-rate brachytherapy was examined. Similar to that observed in the irradiated human breast cancer samples, induction of a Treg but not a $CD8^+$ effector T cell gene signature was detected (Fig. 2G), an observation that reflects previously reported multiplex immunohistochemistry analyses performed on these biopsies.[16]

Radiation-induced Treg responses correlate with widespread differences in innate and adaptive immune responses to RT

As an extension to the preceding analyses, bulk RNA sequencing was performed on the immune compartment of 3 × 4 Gy and 1 × 20 Gy-irradiated AT3-OVA tumors at days 5 and 13 after completion of RT. Mock-irradiated tumors from mice anesthetized as per their irradiated counterparts were used as controls (3 × 0 Gy and 1 × 0 Gy, respectively). By day 5, RT had evoked substantial transcriptional modulation across the immune compartment, but these changes were largely concordant between the 2 schedules (Fig. E4). Transcriptional contrasts between the 2 radiation schedules were revealed when prominent DEGs (adjusted P value <.05 and $\log_2$-fold change >1) were filtered and tested for overrepresented gene ontologies (GO). GO terms overrepresented in 3 × 4 Gy-irradiated tumors covered diverse arms of the immune system relating to T, B, and myeloid cell populations (Fig. 3A, top). In contrast, Treg differentiation and related immunosuppressive signatures were significantly enriched in response to 1 × 20 Gy RT (Fig. 3A, bottom).

Although differences in $CD8^+$ T and NK cell numbers were not observed between the 2 radiation schedules at day 5, enrichment of gene signatures for T, NK cell, and conventional dendritic cell activation, and production of the stimulatory cytokines type I IFN and IFN-γ were consistently higher in 3 × 4 Gy compared with 1 × 20 Gy-irradiated tumors (Fig. 3B). With the contraction of the Treg response by day 13, at which point 3 × 4 Gy-irradiated tumors were escaping but sustained control of 1 × 20 Gy-irradiated tumors was still evident (Fig. 1B-E), most of these signatures were now restricted to 1 × 20 Gy-irradiated tumors (Fig. 3B). Correspondingly, at day 5 after RT, granzyme B expression was significantly elevated within the $CD8^+$ T cell compartment of only 3 × 4 Gy-irradiated tumors (Fig. 3C). Radiation-induced loss of tumor-associated PD-1^+ $CD8^+$ T cells was also most profound in the 1 × 20 Gy-irradiated tumors (Fig. 3D). By day 13, this population of $CD8^+$ T cells had significantly expanded within the irradiated tumors, which correlated with increased expression of granzyme B within the CD8 T compartment (Fig. 3C-D). Notably, these observations were unique to the irradiated tumors; such differences between the 2 radiation schedules were not detected within the inguinal lymph nodes from the same mammary fat pads (Fig. E5) or spleens (data not shown). Within the NK cell compartment of 3 × 4 Gy and 1 × 20 Gy-irradiated tumors at day 5 post-RT, a comparable increase in granzyme B expression was detected relative to mock-irradiated tumors (Fig. 3E), suggesting that RT may enhance the cytotoxic potential of NK cells. However, at day 13 post-RT, NK activation markers including NKG2A and DNAM1 were significantly upregulated in response to 1 × 20 Gy RT relative to mock and 3 × 4 Gy RT (Fig. 3F). Intracellular levels of IFN-y were also only elevated in the NK cell compartment of 1 × 20 Gy-irradiated tumors (Fig. 3F). The observed inverse correlation between radiation-induced Treg response kinetics and activation of T and NK cells suggests that acute Treg responses within irradiated tumors play an important role in shaping concomitant local immunologic processes.

Depletion of tumor-associated Tregs unmasks the immunoadjuvant potential of RT

To determine the extent to which radiation-induced Tregs effect the antitumor activity of the 3 × 4 Gy and 1 × 20 Gy schedules, AT3-OVA tumor cells were injected into DEREG mice, which express a diphtheria toxin (DT) receptor under the control of Foxp3, thus enabling specific Treg depletion after DT administration.[25] A single dose of DT at day 3 after completion of RT, just before the expected rise in tumor-associated Tregs (Fig. 2C), significantly enhanced the antitumor effect of both schedules (Fig. 4A). Similar results were achieved in wildtype mice injected with a Treg-depleting antibody against CTLA-4 (clone 9H10; Fig. 4B).[26] It was confirmed that 9H10 treatment, administered concurrently with RT, selectively prevented the accumulation of Tregs within tumors, with no effect on $CD8^+$ or $CD4^+$ conventional T cells (Fig. E6A). Furthermore, the effect of 9H10 on Tregs was unique to irradiated tumors; Treg numbers remained unaltered in mock-irradiated tumors and in spleens from the same mice (Fig. E6A-B). No single-agent antitumor activity of 9H10 was detected (Fig. 4B). Additionally, $CD8^+$ T and NK cells were critical to the enhanced antitumor activity of RT when given with 9H10 treatment; antibody-mediated depletion of either subset abrogated the therapeutic gain of the combination (Fig. 4B). Similar experiments were run with a nondepleting anti-CTLA-4 antibody (clone 9D9 D265A[15]), in which the 3 × 4 Gy but not 1 × 20 Gy schedule was capable of augmenting the antitumor activity of anti-CTLA-4 therapy in a $CD8^+$ T cell-dependent manner (Fig. E6C). Thus,

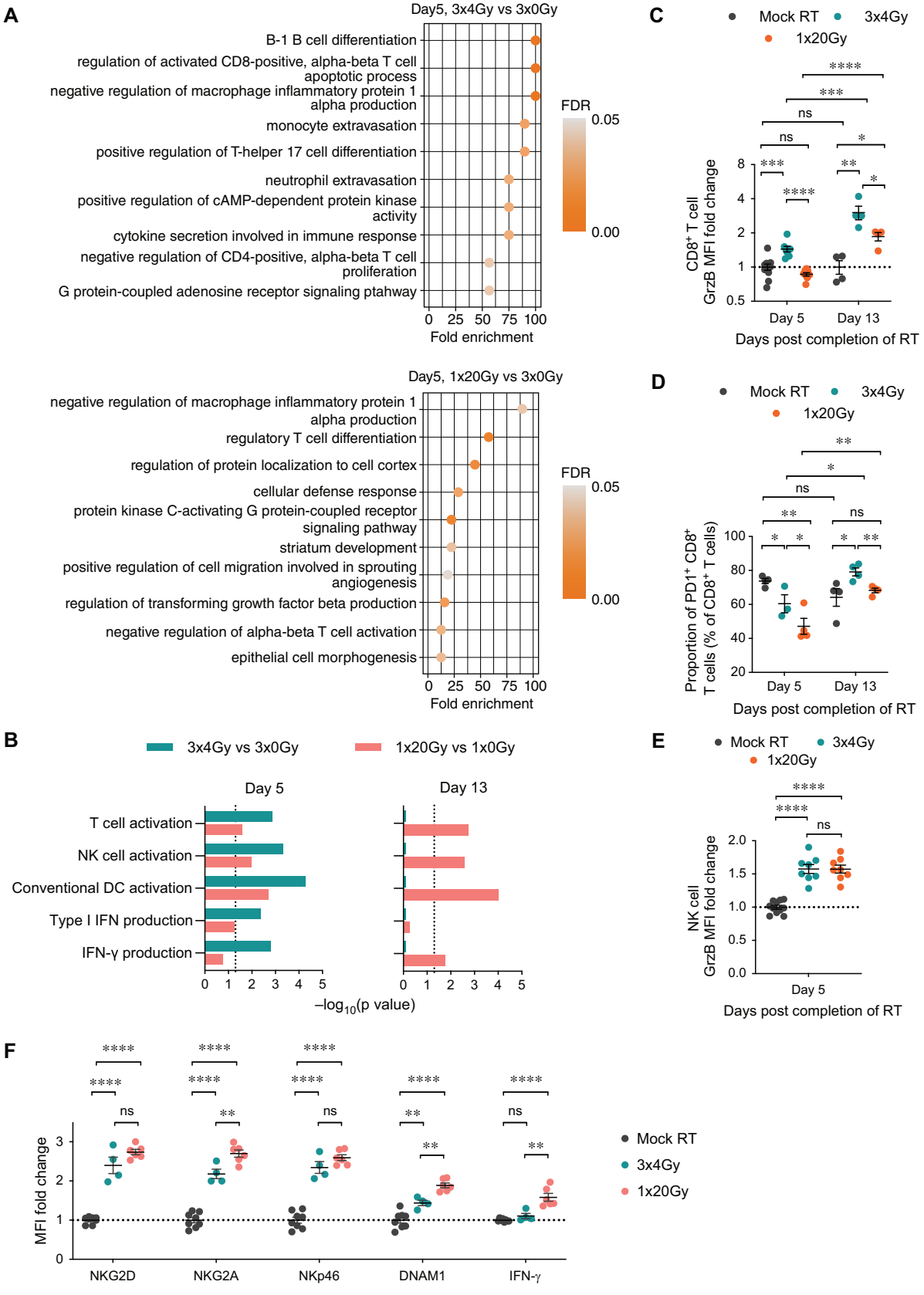

Fig. 3. Heightened expression of Treg-associated gene signatures by 1 × 20 Gy radiation therapy (RT) correlates with delayed local activation of T and natural killer (NK) cell responses relative to 3 × 4 Gy RT. (A) Top GO-BP terms enriched in the immune compartment of AT3-OVA tumors 5 days after RT completion. Bold terms highlight immunosuppressive signatures. FDR = false discovery rate. (B) Enrichment of innate and adaptive immune gene sets at days 5 and 13. Dotted line

depletion of Tregs, not CTLA-4 blockade, markedly improved the immunoadjuvant potential of RT.

Supporting this, although 9H10 treatment did not increase the number of cDC1s within irradiated AT3-OVA tumors (Fig. 4C), it enhanced their maturation status as determined by CD86 expression (Fig. 4D), which correlated with increased granzyme B expression in $CD8^+$ T cells (Fig. 4E). These data suggest that Tregs can limit the immunoadjuvant potential of RT by suppressing cDC1 function. Indeed, a strong negative correlation between the abundance of Tregs relative to that of cDC1s in irradiated tumors (Treg:cDC1 ratio) and the induction of CD86 expression on cDC1s was identified (Fig. 4F). Furthermore, the therapeutic gain of combining 1 × 20 Gy RT with 9H10 treatment in wildtype mice was lost in cDC1-deficient *Batf3*$^{-/-}$ mice (Fig. 4G).

Tumors that do not support radiation-induced Treg responses are vulnerable to the immunoadjuvant effects of 1 × 20 Gy RT

MC38 colon adenocarcinoma tumors were next used to investigate the local immunological impact of RT. In MC38 tumors, $CD8^+$ T and NK cells were critical to the antitumor activity of 1 × 20 Gy RT, as demonstrated by the significant loss of radiation-induced tumor control in mice injected with depleting antibodies against CD8β or asialo-GM1, respectively (Fig. E7A-B). Examination of the immune composition of MC38 tumors after 1 × 20 Gy RT revealed no enrichment of either Tregs or total $CD8^+$ T cells (Fig. E7C). However, an increase in the ratio of $CD8^+$ T cells to Tregs at both days 5 and 10 post-RT was observed (Fig. E7D). These data indicate that not all tumor types are conducive to supporting amplified Treg responses after RT, and such tumors are likely to be highly vulnerable to the immunoadjuvant effects of RT.

Radiation-induced Treg responses restrict the ability of 1 × 20 Gy RT to generate abscopal and immunologic memory responses

To examine the impact of Treg depletion on the abscopal activity of RT, AT3-OVA tumor cells were injected bilaterally into the mammary fat pads of wildtype mice. The 9H10 treatment was started concurrently with the delivery of 1 × 20 Gy RT to only one of these tumors, and growth of the irradiated and unirradiated tumors was monitored (Fig. 5A). Control of tumors outside the irradiated volume was only observed in mice receiving both RT and 9H10 treatment (Fig. 5B), suggesting that localized inhibition of radiation-induced Treg responses can unmask the abscopal activity of high-DPF RT.

To test the potential for the 1 × 20 Gy schedule to also support the induction of memory responses, splenocytes from 9H10-treated wildtype mice bearing irradiated or mock-irradiated AT3-OVA tumors (as described in Fig. 4B) were transferred into treatment-naive wildtype recipients, which were later challenged with either AT3-OVA or AT3-parental tumor inoculums (Fig. 5C). Induction of a memory response that could control AT3-OVA tumors was detected for both radiation schedules (Fig. 5D, left). Cotreatment with 9H10 was critical for the induction of these responses, because splenocytes from 3 × 4 Gy and 1 × 20 Gy-irradiated and control isotype-treated groups could not elicit a response that slowed AT3-OVA tumor growth (Fig. E8). Furthermore, the development of these memory responses was dependent on both $CD8^+$ T and NK cells, as demonstrated by the failure of splenocyte transfers from mice cotreated with depleting antibodies against CD8β or asialo-GM1 to evoke responses to the AT3-OVA tumors (Fig. E8). However, most interesting was the differential ability of the 1 × 20 Gy and 3 × 4 Gy RT-induced memory responses to control AT3-parental tumors (Fig. 5D, right). Only the 1 × 20 Gy schedule was capable of generating a memory response that could significantly slow the growth of AT3-parental tumors, suggesting that high-DPF schedules may be more proficient at evoking a broader repertoire of tumor-reactive memory T cell responses.

Discussion

In this study, we demonstrated that the impact of the 2 major radiation dose-fractionation parameters of DPF and BED on $CD8^+$ T cell-mediated antitumor activity is heavily influenced by radiation-induced Treg responses. In irradiated AT3-OVA tumors, the kinetics and amplitude of Treg accumulation after RT increased in a DPF-dependent manner. Consequently, low-to-moderate DPF schedules (3 × 4 Gy, 9 × 4 Gy, 3 × 8 Gy) were more proficient than high-DPF schedules (1 × 12 Gy, 1 × 20 Gy) at supporting cDC1-dependent stimulation of $CD8^+$ T cell-based antitumor responses and in turn the therapeutic activity of anti-PD-1 therapy. In line with these findings, high-DPF RT failed to induce a $CD8^+$ T effector gene signature in human breast and prostate cancers but did significantly increase their Treg score. In MC38 tumors, in which radiation-induced enrichment of Tregs was not observed, the 1 × 20 Gy schedule was uninhibited in its ability to promote $CD8^+$

represents $P < .05$. (C) and (E) Expression of granzyme B in tumor-associated (C) $CD8^+$ T and (E) NK cells. (D) Proportion of tumor-associated PD-1^+ $CD8^+$ T cells. Data representative of 2 independent experiments. (F) Expression of activation markers and intracellular IFN-γ levels in tumor-associated NK cells at day 13. Data presented as fold change in mean fluorescence intensity (MFI) relative to mock-irradiated controls (dotted line), representative of 2 independent experiments. Data presented as mean ± SEM. *Abbreviation:* NS = nonsignificant. *$P < .05$, **$P < .01$, ***$P < .001$, ****$P < .0001$.

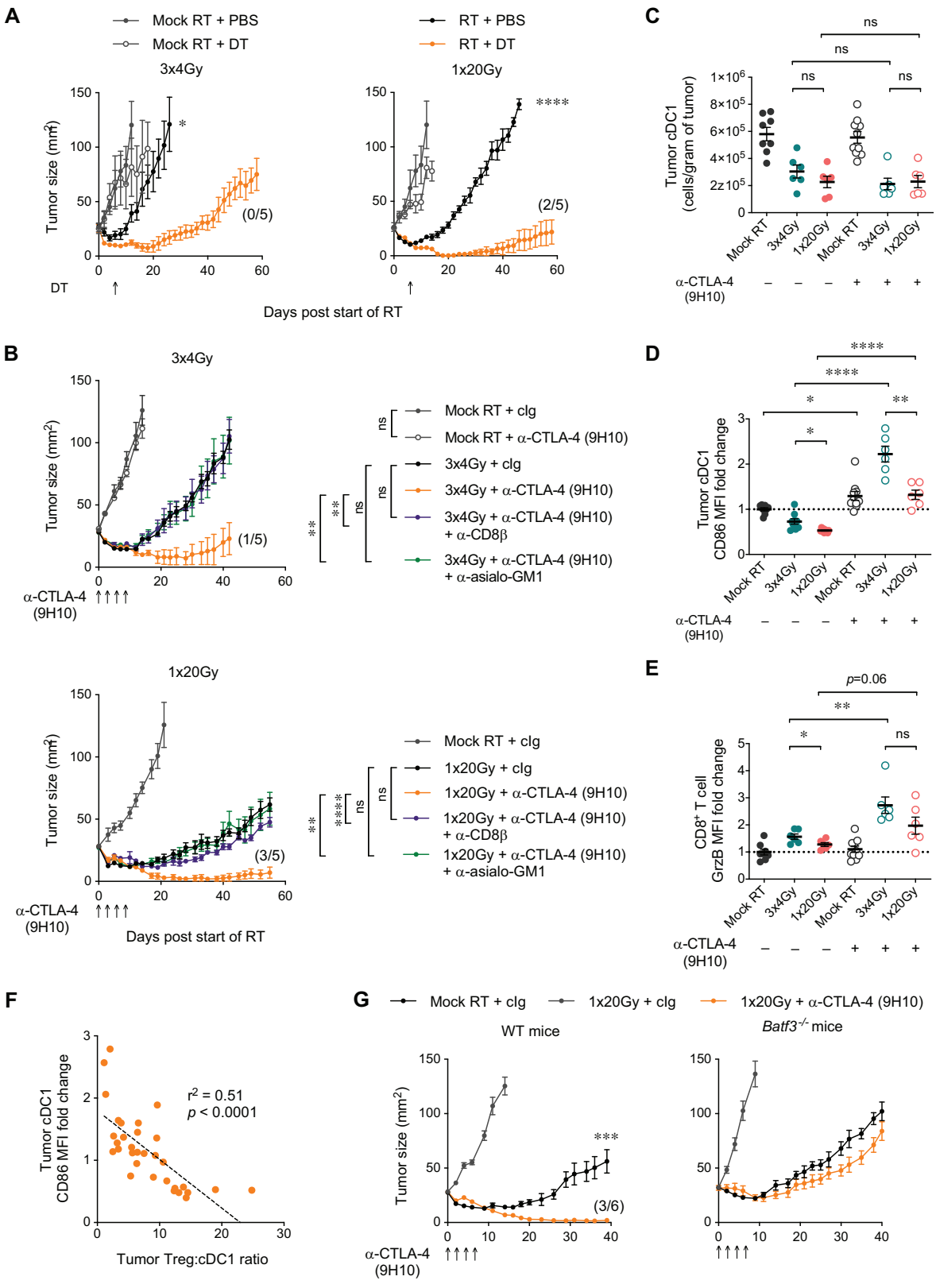

Fig. 4. Tregs negatively effect CD8$^+$ T and NK cell responses to RT. (A, B, and G) Growth of AT3-OVA tumors in (A) DEREG mice treated with diphtheria toxin (DT) or phosphate-buffered saline, as indicated by arrows; (B) wild type (WT) mice treated with anti-CTLA-4 therapy (9H10) or control isotype, as indicated by arrows, in conjunction with anti-CD8β or anti-asialo-GM1 antibodies; (G) WT and *Batf3*$^{-/-}$ mice treated with anti-CTLA-4 antibodies (9H10) or control isotype, as indicated by arrows. n = 4 to 6 mice/group, data representative of 2 independent experiments. Numbers in parentheses indicate

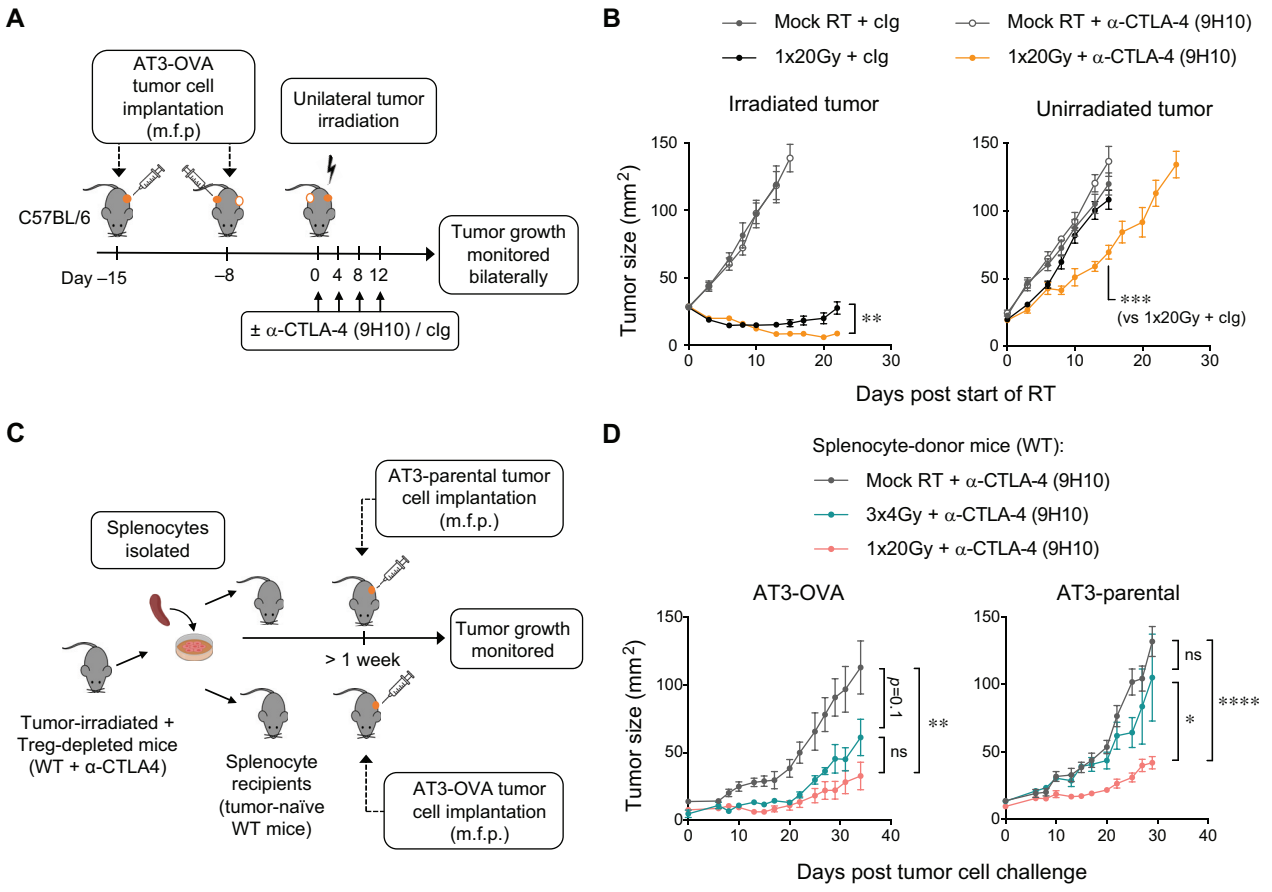

Fig. 5. Treg depletion in conjunction with RT is critical for the development of abscopal and memory responses. (A) Schema of experimental approach (abscopal response). (B) Growth of irradiated and unirradiated (distant) AT3-OVA tumors in wild type (WT) mice treated with anti-CTLA-4 (9H10) antibodies or control isotype. n = 6 to 8 mice/group. (C) Schema of experimental approach (memory response). (D) Growth of AT3-OVA and AT3-parental tumors in WT mice transplanted with splenocytes from anti-CTLA-4-treated WT mice bearing irradiated or mock-irradiated tumors. n = 4 to 6 mice/group. Data representative of 2 independent experiments. Data presented as mean ± standard error of the mean. *Abbreviation:* NS = nonsignificant. *$P < .05$, **$P < .01$, ***$P < .001$, ****$P < .0001$.

T and NK cell−mediated tumor control. A similar outcome was achieved in AT3-OVA tumors with the targeted inhibition of radiation-induced Treg responses. Together, these findings point to Tregs as a critical determinant of radiation-induced antitumor immunity. Because Treg responses within irradiated tumors are influenced by both radiation dose fractionation and tumor type, this may in part account for the heterogeneous nature of immune responses to RT observed across the clinical landscape.[27]

Although the effects of RT on Tregs have been documented across various murine and human tumors,[16,28-32] herein we have highlighted the differential effects of radiation dose fractionation and tumor type on Treg responses. Moreover, our study findings suggest that for certain tumors, the success of immunotherapeutic agents not targeted at the Treg compartment (ie, anti-PD-1 and nondepleting anti-CTLA-4 antibodies) could be significantly influenced by the DPF of the radiation schedule used. Landmark work by Vanpouille-Box et al showed that tumor cell −intrinsic regulators of immunogenicity were an important determinant of a radiation schedule's immunoadjuvant potential.[7] Treatments of 8 Gy per fraction or less were

fraction of tumor-free mice at days (A) 90, (B) 50, and (G) 40 after the start of RT. (C) Absolute numbers of cDC1s in irradiated AT3-OVA tumors harvested from wildtype mice treated with anti-CTLA-4 therapy or isotype control, at day 5. (D and E) CD86 expression on cDC1s and (E) granzyme B expression in $CD8^+$ T cells from irradiated AT3-OVA tumors harvested from WT mice treated with anti-CTLA-4 antibodies or isotype control, at day 5. Data presented relative to mock-irradiated and isotype-treated controls (dotted line). Data in (A-E) and (G) are presented as mean ± standard error of the mean. *$P <$ .05, **$P < .01$, ***$P < .001$, ****$P < .0001$. (F) Correlation between the ratio of tumor-associated Treg:cDC1 numbers and the induction of CD86 on cDC1s (expressed as fold change over respective control groups) across all irradiated tumors ± anti-CTLA-4 therapy. The R^2 goodness-of-fit and P values in linear regression analysis are displayed.

more effective than a single fraction of 20 Gy at activating the STING/type I IFN signaling pathway and abscopal responses that could support the antitumor activity of checkpoint blockade immunotherapy.[5,7] However, in the AT3-OVA tumor model, depletion of tumor-associated Tregs was sufficient to unmask the ability of the 1 × 20 Gy schedule to evoke $CD8^+$ T and NK cell responses that were equivalent to those observed for the 3 × 4 Gy schedule, resulting in tumor cure and the induction of abscopal responses and immunologic memory. In line with these findings, inhibition of the adenosinergic pathway by targeted blocking of CD73 -in irradiated TSA and 4T1 tumors has been shown to enhance the immunoadjuvant potential of 1 × 20 Gy RT, an effect that was also associated with reduced enrichment of tumor-associated Tregs and increased cDC1 maturation.[33] Thus, both tumor cells and stroma are likely to be equally critical players underpinning the differential impact of radiation dose fractionation on host antitumor immune defenses.

The kinetics and amplitude of T and NK cell responses within 3 × 4 Gy and 1 × 20 Gy-irradiated tumors were highly comparable during the first 2 weeks after completion of RT, although recovery of tumor-associated $PD\text{-}1^+$ $CD8^+$ T cells was more delayed after 1 × 20 Gy RT. The functional status of the $CD8^+$ T cell compartment in 1 × 20 Gy-irradiated tumors, as read out by granzyme B expression, was also significantly restrained by the heightened Treg response. Together, these factors likely reduced the window of opportunity for the 1 × 20 Gy radiation schedule to synergize with anti-PD-1 therapy. Enrichment of the immunosuppressive cytokine TGF-β within only the 1 × 20 Gy-irradiated tumors was explored as a possible contributing factor to the heightened recruitment or expansion of tumor-associated Tregs, relative to that observed in 3 × 4 Gy and 9 × 4 Gy-irradiated tumors. Mice were treated with TGF-β blocking antibodies, but this failed to limit the Treg response to 1 × 20 Gy RT (data not shown). In a recent study by De Martino et al,[34] tumor cell secretion of activin A (a member of the TGF-β superfamily)[35] was shown to be induced by RT and to negate the ability of TGF-β-targeted drugs to block Treg recruitment into irradiated tumors. Investigations are ongoing to determine whether AT3-OVA tumor cells are a source of activin A, but because baseline tumor cell−intrinsic levels of activin A are likely to differ across tumor types, this may in part account for the differential ability of AT3-OVA and MC38 tumors to support radiation-induced Treg responses, irrespective of tissue niche. Ultimately, the identification of tumor-associated factors predictive of radiation-induced Treg responses will help in the design of more tailored RT-immunotherapy approaches.

In addition to examining the local impact of radiation-induced Treg responses on the tumor immune microenvironment, we also demonstrated that Treg responses within irradiated tumors are a dominant barrier to the genesis of abscopal responses and systemic immunologic memory. Despite the ability of the 3 × 4 Gy schedule to evoke $CD8^+$ T cell responses that could control AT3-OVA tumors independent of immunotherapy, it was ineffective at establishing a memory response that could be recalled upon re-exposure to AT3-OVA tumor cells. This was only achieved in mice cotreated with RT and a Treg-depleting agent. Comparison of the 1 × 20 Gy and 3 × 4 Gy schedules revealed that only 1 × 20 Gy RT could evoke memory responses against both AT3-OVA and AT3-parental tumors, indicative of the enhanced capability of this radiation schedule to alter the antigenicity of tumors and in turn broaden the TCR repertoire of the responding T cell pool. Notably, in the clinic, SABR schedules have also been reported to increase the diversity of peripheral and tumor-infiltrating T cell clones with and without concurrent immunotherapy.[36-38]

Based on the local effects of combining RT and 9H10 (Treg-depleting anti-CTLA-4 therapy), we predict that local Treg depletion could equalize the impact of DPF and BED on radiation abscopal activity. The observed similarity in memory responses against the AT3-OVA tumors after cotreatment with 3 × 4 Gy or 1 × 20 Gy RT and 9H10 supports this hypothesis. However, Dewan et al and Vanpouille-Box et al were able to highlight differential effects of radiation dose fractionation on the abscopal activity of RT in TSA tumor-bearing mice in the context of 9H10 treatment.[5,7] These seminal findings have in part led to the common use of the 3 × 8 Gy schedule with immune checkpoint inhibitors in human trials, which have shown promising heightened immunologic responses,[39,40] although not consistently across all studies.[41,42] Differences between the C56BL/6 AT3-OVA and Balb/c TSA tumor models, most notably their genetic backgrounds[43] and stromal cell composition of the tumor microenvironment,[44,45] are likely to account for the differential sensitivity of abscopal responses to 9H10 treatment.

Conclusions

Overall, this study represents an important preclinical interrogation of the immunomodulatory effects of radiation dose fractionation and is one of the few to examine such effects independently of immunotherapy. It can be envisaged from the findings presented that strategies to predict or eliminate radiation-induced Treg responses will solidify the positioning of RT as a key adjuvant in the immuno-oncology era.

References

1. Rodriguez-Ruiz ME, Vitale I, Harrington KJ, Melero I, Galluzzi L. Immunologic impact of cell death signaling driven by radiation on the tumor microenvironment. *Nat Immunol* 2020;21:120–134.
2. Spiotto M, Fu YX, Weichselbaum RR. The intersection of radiotherapy and immunotherapy: Mechanisms and clinical implications. *Sci Immunol* 2016;1.

3. Pan H, Simpson DR, Mell LK, Mundt AJ, Lawson JD. A survey of stereotactic body radiotherapy use in the United States. *Cancer* 2011;117:4566–4572.
4. Lund CR, Cao JQ, Liu M, Olson R, Halperin R, Schellenberg D. The distribution and patterns of practice of stereotactic ablative body radiotherapy in Canada. *J Med Imaging Radiat Sci* 2014;45:8–15.
5. Dewan MZ, Galloway AE, Kawashima N, et al. Fractionated but not single-dose radiotherapy induces an immune-mediated abscopal effect when combined with anti-CTLA-4 antibody. *Clin Cancer Res* 2009;15:5379–5388.
6. Grapin M, Richard C, Limagne E, et al. Optimized fractionated radiotherapy with anti-PD-L1 and anti-TIGIT: A promising new combination. *J Immunother Cancer* 2019;7:160.
7. Vanpouille-Box C, Alard A, Aryankalayil MJ, et al. DNA exonuclease Trex1 regulates radiotherapy-induced tumour immunogenicity. *Nat Commun* 2017;8 15618.
8. Harding SM, Benci JL, Irianto J, Discher DE, Minn AJ, Greenberg RA. Mitotic progression following DNA damage enables pattern recognition within micronuclei. *Nature* 2017;548:466–470.
9. Burnette BC, Liang H, Lee Y, et al. The efficacy of radiotherapy relies upon induction of type I interferon-dependent innate and adaptive immunity. *Cancer Res* 2011;71:2488–2496.
10. Deng L, Liang H, Xu M, et al. STING-dependent cytosolic DNA sensing promotes radiation-induced type I interferon-dependent antitumor immunity in immunogenic tumors. *Immunity* 2014;41:843–852.
11. Schadt L, Sparano C, Schweiger NA, et al. Cancer-cell-intrinsic cGAS expression mediates tumor immunogenicity. *Cell Rep* 2019;29 1236-1248 e7.
12. Stewart TJ, Abrams SI. Altered immune function during long-term host-tumor interactions can be modulated to retard autochthonous neoplastic growth. *J Immunol* 2007;179:2851–2859.
13. Mattarollo SR, Loi S, Duret H, Ma Y, Zitvogel L, Smyth MJ. Pivotal role of innate and adaptive immunity in anthracycline chemotherapy of established tumors. *Cancer Res* 2011;71:4809–4820.
14. Franken NA, Rodermond HM, Stap J, Haveman J, van Bree C. Clonogenic assay of cells in vitro. *Nat Protoc* 2006;1:2315–2319.
15. Selby MJ, Engelhardt JJ, Quigley M, et al. Anti-CTLA-4 antibodies of IgG2a isotype enhance antitumor activity through reduction of intratumoral regulatory T cells. *Cancer Immunol Res* 2013;1:32–42.
16. Keam SP, Halse H, Nguyen T, et al. High dose-rate brachytherapy of localized prostate cancer converts tumors from cold to hot. *J Immunother Cancer* 2020;8 e000792.
17. Fowler JF. 21 years of biologically effective dose. *Br J Radiol* 2010;83:554–568.
18. Verbrugge I, Hagekyriakou J, Sharp LL, et al. Radiotherapy increases the permissiveness of established mammary tumors to rejection by immunomodulatory antibodies. *Cancer Res* 2012;72:3163–3174.
19. Hildner K, Edelson BT, Purtha WE, et al. Batf3 deficiency reveals a critical role for CD8alpha+ dendritic cells in cytotoxic T cell immunity. *Science* 2008;322:1097–1100.
20. Weiss JM, Bilate AM, Gobert M, et al. Neuropilin 1 is expressed on thymus-derived natural regulatory T cells, but not mucosa-generated induced Foxp3+ T reg cells. *J Exp Med* 2012;209:1723–1742 S1..
21. Yadav M, Louvet C, Davini D, et al. Neuropilin-1 distinguishes natural and inducible regulatory T cells among regulatory T cell subsets in vivo. *J Exp Med* 2012;209:1713–1722 , S1-19.
22. Horton JK, Siamakpour-Reihani S, Lee CT, et al. FAS death receptor: A breast cancer subtype-specific radiation response biomarker and potential therapeutic target. *Radiat Res* 2015;184:456–469.
23. Zemmour D, Zilionis R, Kiner E, Klein AM, Mathis D, Benoist C. Single-cell gene expression reveals a landscape of regulatory T cell phenotypes shaped by the TCR. *Nat Immunol* 2018;19:291–301.
24. Spranger S, Dai D, Horton B, Gajewski TF. Tumor-residing Batf3 dendritic cells are required for effector T Cell trafficking and adoptive T cell therapy. *Cancer Cell* 2017;31 711-723 e4.
25. Lahl K, Sparwasser T. In vivo depletion of FoxP3+ Tregs using the DEREG mouse model. *Methods Mol Biol* 2011;707:157–172.
26. Simpson TR, Li F, Montalvo-Ortiz W, et al. Fc-dependent depletion of tumor-infiltrating regulatory T cells co-defines the efficacy of anti-CTLA-4 therapy against melanoma. *J Exp Med* 2013;210:1695–1710.
27. Ko EC, Formenti SC. Radiotherapy and checkpoint inhibitors: A winning new combination? *Ther Adv Med Oncol* 2018;10 1758835918768240.
28. Persa E, Balogh A, Safrany G, Lumniczky K. The effect of ionizing radiation on regulatory T cells in health and disease. *Cancer Lett* 2015;368:252–261.
29. Muroyama Y, Nirschl TR, Kochel CM, et al. Stereotactic radiotherapy increases functionally suppressive regulatory T cells in the tumor microenvironment. *Cancer Immunol Res* 2017;5:992–1004.
30. Bos PD, Plitas G, Rudra D, Lee SY, Rudensky AY. Transient regulatory T cell ablation deters oncogene-driven breast cancer and enhances radiotherapy. *J Exp Med* 2013;210:2435–2466.
31. Sharabi AB, Nirschl CJ, Kochel CM. Stereotactic radiation therapy augments antigen-specific PD-1-mediated antitumor immune responses via cross-presentation of tumor antigen. *Cancer Immunol Res* 2015;3:345–355.
32. Schaue D, Ratikan JA, Iwamoto KS, McBride WH. Maximizing tumor immunity with fractionated radiation. *Int J Radiat Oncol Biol Phys* 2012;83:1306–1310.
33. Wennerberg E, Spada S, Rudqvist NP, et al. CD73 blockade promotes dendritic cell infiltration of irradiated tumors and tumor rejection. *Cancer Immunol Res* 2020;8:465–478.
34. De Martino M, Daviaud C, Diamond JM, et al. Activin A promotes regulatory T-cell-mediated immunosuppression in irradiated breast cancer. *Cancer Immunol Res* 2021;9:89–102.
35. Loomans HA, Andl CD. Activin receptor-like kinases: A diverse family playing an important role in cancer. *Am J Cancer Res* 2016;6:2431–2447.
36. Twyman-Saint Victor C, Rech AJ, Maity A, et al. Radiation and dual checkpoint blockade activate non-redundant immune mechanisms in cancer. *Nature* 2015;520:373–377.
37. Rudqvist NP, Pilones KA, Lhuillier C, et al. Radiotherapy and CTLA-4 blockade shape the TCR repertoire of tumor-infiltrating T cells. *Cancer Immunol Res* 2018;6:139–150.
38. Phillips R, Shi WY, Deek M, et al. Outcomes of observation vs stereotactic ablative radiation for oligometastatic prostate cancer: The ORIOLE phase 2 randomized clinical trial. *JAMA Oncol* 2020;6:650–659.
39. Formenti SC, Rudqvist NP, Golden E, et al. Radiotherapy induces responses of lung cancer to CTLA-4 blockade. *Nat Med* 2018;24:1845–1851.
40. Theelen W, Peulen HMU, Lalezari F, et al. Effect of pembrolizumab after stereotactic body radiotherapy vs pembrolizumab alone on tumor response in patients with advanced non-small cell lung cancer: Results of the PEMBRO-RT phase 2 randomized clinical trial. *JAMA Oncol* 2019;5:1276–1282.
41. Voorwerk L, Slagter M, Horlings HM, et al. Immune induction strategies in metastatic triple-negative breast cancer to enhance the sensitivity to PD-1 blockade: The TONIC trial. *Nat Med* 2019;25:920–928.
42. McBride S, Sherman E, Tsai CJ, et al. Randomized phase II trial of nivolumab with stereotactic body radiotherapy versus nivolumab alone in metastatic head and neck squamous cell carcinoma. *J Clin Oncol* 2021;39:30–37.
43. Foerster F, Boegel S, Heck R, et al. Enhanced protection of C57 BL/6 vs Balb/c mice to melanoma liver metastasis is mediated by NK cells. *Oncoimmunology* 2018;7 e1409929.
44. Sakaguchi S, Yamaguchi T, Nomura T, Ono M. Regulatory T cells and immune tolerance. *Cell* 2008;133:775–787.
45. Turley SJ, Cremasco V, Astarita JL. Immunological hallmarks of stromal cells in the tumour microenvironment. *Nat Rev Immunol* 2015;15:669–682.

Author/s:
Sia, J; Hagekyriakou, J; Chindris, I; Albarakati, H; Leong, T; Schlenker, R; Keam, SP; Williams, SG; Neeson, PJ; Johnstone, RW; Haynes, NM

Title:
Regulatory T Cells Shape the Differential Impact of Radiation Dose-Fractionation Schedules on Host Innate and Adaptive Antitumor Immune Defenses

Date:
2021-10-01

Citation:
Sia, J., Hagekyriakou, J., Chindris, I., Albarakati, H., Leong, T., Schlenker, R., Keam, S. P., Williams, S. G., Neeson, P. J., Johnstone, R. W. & Haynes, N. M. (2021). Regulatory T Cells Shape the Differential Impact of Radiation Dose-Fractionation Schedules on Host Innate and Adaptive Antitumor Immune Defenses. INTERNATIONAL JOURNAL OF RADIATION ONCOLOGY BIOLOGY PHYSICS, 111 (2), pp.502-514. https://doi.org/10.1016/j.ijrobp.2021.05.014.

Persistent Link:
http://hdl.handle.net/11343/280669

File Description:
Published version